ISSN 0006-2979, Biochemistry (Moscow), 2023, Vol. 88, No. 10, pp. 1513-1527 © Pleiades Publishing, Ltd., 2023.
Russian Text © The Author(s), 2023, published in Biokhimiya, 2023, Vol. 88, No. 10, pp. 1829-1846.

REVIEW

Investigation of the Mechanism of Membrane Potential Generation by Heme-Copper Respiratory Oxidases in a Real Time Mode

Sergei A. Siletsky

Belozersky Institute of Physico-Chemical Biology, Lomonosov Moscow State University, 119991 Moscow, Russia

e-mail: siletsky@belozersky.msu.ru

Received June 29, 2023
Revised August 15, 2023
Accepted August 15, 2023

Abstract—Heme-copper respiratory oxidases are highly efficient molecular machines. These membrane enzymes catalyze the final step of cellular respiration in eukaryotes and many prokaryotes: the transfer of electrons from cytochromes or quinols to molecular oxygen and oxygen reduction to water. The free energy released in this redox reaction is converted by heme-copper respiratory oxidases into the transmembrane gradient of the electrochemical potential of hydrogen ions ($\Delta\mu H^+$). Heme-copper respiratory oxidases have a unique mechanism for generating $\Delta\mu H^+$, namely, a redox-coupled proton pump. A combination of direct electrometric method for measuring the kinetics of membrane potential generation with the methods of prestationary kinetics and site-directed mutagenesis in the studies of heme-copper oxidases allows to obtain a unique information on the translocation of protons inside the proteins in real time. The review summarizes the data of studies employing time-resolved electrometry to decipher the mechanisms of functioning of these important bioenergetic enzymes.

DOI: 10.1134/S0006297923100085

Keywords: bioenergetics, cytochrome oxidase, proteoliposomes, electrogenic proton transfer, $\Delta\Psi$ generation, proton pump, photoreduction, cytochrome aa_3, kinetics, direct electrometric method, capacitive potentiometry, time resolution, zinc ions

INTRODUCTION. HEME-COPPER RESPIRATORY OXIDASES

Terminal respiratory oxidases are key components of respiratory chains of the mitochondria and most aerobic bacteria [1, 2]. These ubiquitous enzymes are at the end of the respiratory chain and catalyze reduction of molecular oxygen by cytochrome *c* or ubiquinol. This process is coupled with the formation of proton motive force (PMF), a transmembrane gradient of the electrochemical potential of hydrogen ions ($\Delta\mu H^+$) [3-7] used as an energy source for various energy-demanding cellular processes, such as membrane transport, synthesis of biomolecules, movement of bacterial cells, etc.

Terminal respiratory oxidases are typically classified into two superfamilies: heme-copper oxidases and cytochromes *bd* [7]. A characteristic feature of heme-copper oxidases is the presence of the oxygen-reducing catalytic site (the so-called binuclear center, BNC) formed by closely located iron ion of the heme group and copper ion. Mitochondrial cytochrome *c* oxidase contains four redox centers (Fig. 1). Its catalytic site is located inside the enzyme hydrophobic core and consists of two redox centers: high-spin heme a_3 iron and copper ion Cu_B. Four electrons supplied by cytochrome *c* through two other redox centers (Cu_A and low-spin heme *a*) sequentially enter the BNC, which ultimately results in the reduction of one oxygen molecule to two water molecules.

Abbreviations: $\Delta\Psi$, transmembrane electrical potential difference; $\Delta\mu H^+$, transmembrane gradient of the electrochemical potential of hydrogen ions; BNC, binuclear center; COX, cytochrome oxidase; F, O, O_H, P, E, E_H, and R, cytochrome *c* oxidase states; P and N sides of the membrane, positively and negatively charged, respectively, aqueous phases separated by the coupling membrane; PLS, proton loading site; Rubpy, tris(bipyridine)ruthenium complex.

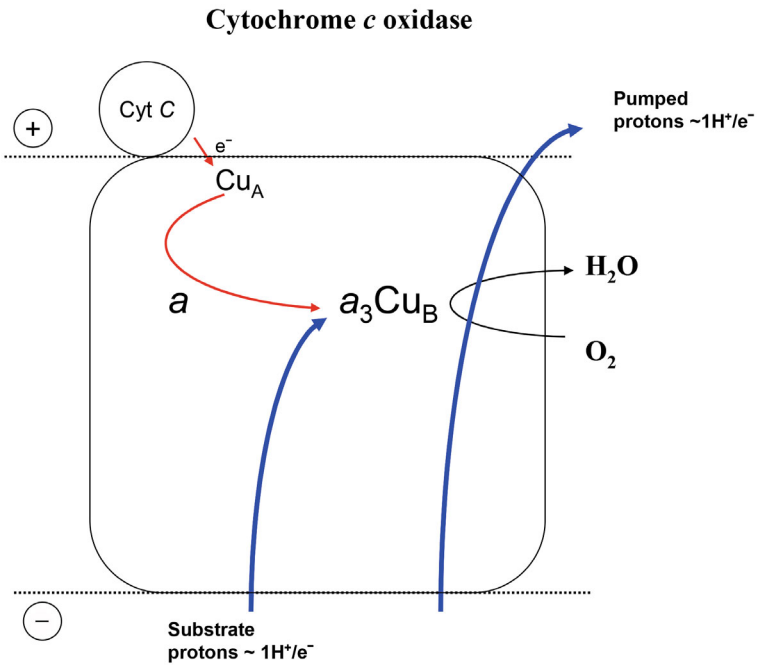

Fig. 1. Scheme of cytochrome oxidase (COX) activity. Negatively and positively charged sides of the membrane face the mitochondrial matrix and the intermembrane space, respectively. In the case of prokaryotic enzymes, the corresponding sides of the membrane face the cytoplasm and the periplasmic space. Red and blue arrows indicate the transfer of electrons and protons, respectively.

In bacterial oxidases, the low-spin heme *a* can be replaced by heme *b*, and the high-spin heme a_3 can be replaced by hemes o_3 or b_3. Some bacterial oxidases have additional heme *c* centers.

The superfamily of heme-copper oxidases includes three large groups: families A, B, and C [8]. Structural modeling and comparative analysis of genomes have identified genes of five new families of terminal oxidases (D, E, F, G, and H) in archaebacteria [5]. Family A has the largest number of representatives and contains the most studied enzymes, including cytochrome oxidases (COXs) from the bovine cardiac muscle mitochondria and yeast, aa_3-type COXs from *Paracoccus denitrificans* and *Rhodobacter sphaeroides*, caa_3 oxidase from *Thermus thermophiles*, and *bo*-type quinol oxidase from *Escherichia coli* [9-17]. A typical representative of the much less studied family B is ba_3-type COX from *T. thermophilus*, which shows low amino acid sequence homology with family A enzymes [18, 19]. The most evolutionary distant family C includes cbb_3 oxidases from various organisms [20, 21].

COX generates the PMF due to the vectorial (across the membrane) delivery of electrons and protons necessary for the catalytic reduction of oxygen to water in the BNC. The so-called chemical (or substrate) protons are transferred to the BNC from the internal aqueous phase (negatively charged N side of the membrane), while electrons are transferred from cytochrome *c* from the positive outer side of the membrane (P side) (Fig. 1, [22]). COX also transfers an average of 4 protons (pumped protons) from the N side to the P side per each reduced oxygen molecule, i.e., functions as a proton pump [23, 24]. Therefore, the reaction catalyzed by COX is associated with a charge separation corresponding to the directed transmembrane transfer of 8 charges per each reduced oxygen molecule and can be described by equation (1):

$$4\,c^{2+} + O_2 + 8H^+_n \rightarrow 4c^{3+} + 2H_2O + 4H^+_p, \qquad (1)$$

where n is the mitochondrial matrix and p is the intermembrane space.

Generation of the membrane potential in a stationary mode (i.e., with multiple enzyme turnovers) by the mitochondrial COX integrated into proteoliposomes was demonstrated in the laboratory of Drachev in the early experiments on the development of direct electrometric method [25]. However, these studies failed to reveal the electrogenic mechanism of membrane potential generation and formation of $\Delta\mu H^+$ in the enzyme catalytic cycle. Later advancements in the development of direct electrometric method with the time resolution adequate for studying the events of the catalytic cycle of photoactive proteins [26] have been successfully used to investigate the activity mechanisms of heme-copper oxidases. Since these enzymes are not photoactivatable proteins, a new methodological approach has been created to study their electrogenic mechanisms with a high time resolution (see below) based on a combination of direct electrometry and special photoactivatable chemical reactions induced by nanosecond laser pulses to trigger electron and proton transfer in COX. This method allows to obtain unique information on the structure and functioning

of the redox-dependent COX proton pump, as well as on the coupling mechanism and stages of proton translocation in the protein in real time (prestationary mode) [27-31].

THREE-DIMENSIONAL STRUCTURE OF COX

X-ray diffraction analysis has been used to establish the three-dimensional structures of several typical heme-copper terminal oxidases of the A family, including COX from the bovine heart mitochondria [32-35], bacterial COXs of the aa_3 type from *P. denitrificans* [36-38] and *R. sphaeroides* [39, 40], and quinol oxidase bo_3 from *E. coli* [41] and COX caa_3 from *T. thermophiles* [42]. Atomic structures have also been obtained for the members of the B and C families, such as cytochrome ba_3 from *T. thermophilus* [19, 43] and COX cbb_3 from *Pseudomonas shutzeri* [21], respectively.

Heme-copper oxidases are characterized by the largest central subunit I consisting of 12 transmembrane α-helices. While bacterial COXs contain no more than 4 subunits, COX from mammalian mitochondria is composed of 13 subunits; its molecular weight (~200 kDa) is approximately twice as large as that of bacterial enzymes. The three largest subunits of mitochondrial COX are encoded by the mitochondrial genome. They form the catalytic core of the enzyme and are homologous to the three main subunits found in most typical prokaryotic family A aa_3 type COXs of the superfamily of heme-copper oxidases.

All family A COXs contain two potential proton pathways (from the internal aqueous phase towards the BNC) that involve conserved proton-exchanging amino acid residues and bound water molecules [19, 32, 36, 39, 42]. Proton pathway D (D channel) [30-32] leads from the D132 residue through a chain of water molecules and amino acid residues bound by hydrogen bonds to the conserved E286 residue located 10-12 Å from the BNC and 24-26 Å from D132 [24-26]. Water molecules in the channel are stabilized through the hydrogen bonds formed with highly conserved hydrophilic amino acid residues (N139, N121, N207, S142, S200, S201, and S197) [33]. Proton pathway K (K channel) [44-46] is located directly below the BNC and leads from the protein surface on the membrane N side through T352, T359, K362, and bound water to Y288 located near the BNC. The entrance to the K channel is formed with the involvement of the E101 residue of the second subunit I [38, 47]. The chain of hydrogen bonds is interrupted between the K362 and T359 residues. It is believed that changes in the K362 conformation restore the chain of hydrogen bonds, ensuring controlled proton transfer [38, 48].

The hydrophilic domain, which is located above the heme groups and Cu_B, can theoretically provide the exit of the pumped proton from the membrane outer side to the aqueous phase [49]. This domain contains a cluster of negatively charged amino acids (including conserved D399 and D404 residues), several arginine residues, propionate substituents of the heme, water molecules, and bound redox-inactive metal atom (Mg^{2+} in the mitochondrial COX that is partially replaced by Mn^{2+} in prokaryotic enzymes) [38]. The transfer of molecular oxygen in the BNC toward the active site occurs through several hydrophobic channels in the middle part of the membrane bilayer [32, 39, 50, 51]. The release of water molecules formed in the BNC presumably takes place at the membrane P side, above the heme groups, in the area of contact between subunits I and II, near the Mg^{2+}/Mn^{2+} site [52].

COX CATALYTIC CYCLE INTERMEDIATES

The catalytic cycle of family A COXs is characterized by two phases, namely, oxidation and reduction half-reactions (Fig. 2), each including two single-electron transitions [53]. During the reduction phase (O → E and E → R transitions), the first two electrons are transferred to the BNC; as a result, it acquires the ability to bind molecular oxygen. The oxidative phase begins with the interaction of reduced BNC (state R; Fig. 2) with an oxygen molecule with the formation of primary diatomic oxygen adduct (state A; not shown in Fig. 2) [54]. The oxygen molecule is transferred through Cu_B to the central iron atom of the high-spin heme a_3 with the generation of the oxycomplex [55], which is a mixture of the $Fe^{2+}-O_2$ and $Fe^{3+}-O_2^-$ states [56]. At the next stage, the interatomic O–O bond is broken and the P_M state is formed (Fig. 2), which requires the transfer to O_2 of at least one proton and four electrons from the active site [57, 58]. Two electrons are supplied during oxidation of the heme a_3 Fe^{2+} ion to the oxoferryl state $Fe^{4+}=O^{2-}$. One electron comes from Cu_B^+ that is oxidized to Cu_B^{2+}. The fourth electron and the proton come from the closely located conserved Y288 residue [59] that forms a covalent bond with the histidine ligand of Cu_B [33, 60, 61]. By donating an electron and a proton, Y288 is converted into a radical [62].

Single-electron reduction of the P_M intermediate converts COX to the F state (transfer of the third electron to Y288). Oxidation of the fourth cytochrome *c* molecule and transfer of the fourth electron to the BNC completes the catalytic cycle with the formation of fully oxidized O_H state (Fig. 2). In the absence of electron donors, the oxidized "unrelaxed" O_H state spontaneously converts to the oxidized stable state (O) within a few seconds. The O and O_H states differ in the electron affinity of their redox centers, as well as in the ability for the transmembrane proton transfer [11, 29, 63-66]. Using the treatment with hydrogen peroxide or carbon monoxide, almost

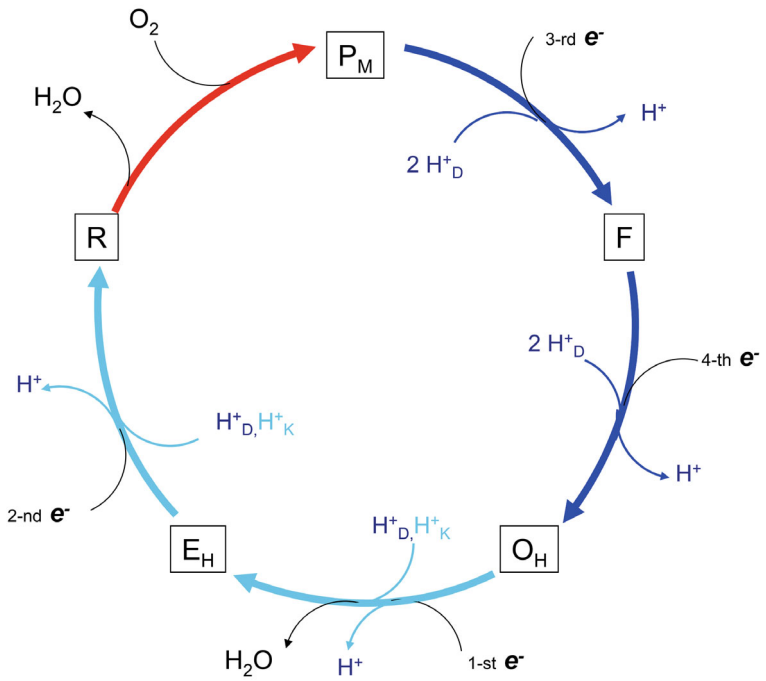

Fig. 2. Catalytic cycle of family A COX enzymes. Transitions R → O_H and O_H → R form, respectively, the oxidative and reduction phases of the catalytic cycle. During the R → P_M transition (red arrow), O_2 molecule binds to heme a_3 of the BNC in the completely reduced Fe^{2+} Cu_B^{1+} state, the O–O bond breaks, and the heme a_3 oxoferryl complex $Fe^{4+}=O^{2-}$ and Cu_B^{1+}-O_H^- is formed. Transitions P_M → F, F → O_H, O_H → E_H, and E_H → R (blue and blue-green arrows) involve sequential transfer of four electrons into the BNC and pumping of protons.

entire enzyme population can be transferred to the stationary states P_M or F that correspond to the partial reduction of molecular oxygen in the BNC with two or three electrons.

TIME-RESOLVED METHODS FOR STUDYING CHARGE TRANSFER IN COX

In direct electrometry, proteoliposomes with a protein under study are attached to an artificial macroscopic membrane (collodium film impregnated with a phospholipid solution in decane) and the transmembrane potential generation kinetics is recorded with a submicrosecond time resolution using macroscopic AgCl electrodes. The difference of the transmembrane electrical potentials ($\Delta\Psi$) on the measured macroscopic membrane increases proportionally to the generation of electrical potential difference on the proteoliposome membrane, which makes it possible to monitor the kinetics of electrogenic translocation of charges in the studied protein with an adequate time resolution in the prestationary mode [26, 67, 68].

The catalytic cycle of COX occurs on a millisecond time scale and involves a sequence of intermediate states of the oxygen-reducing BNC, as well as individual electron and proton transfer events within transitions between the BNC intermediate states. All of these reactions occur faster than the time resolution limits of fast mixing methods. To study the catalytic cycle of COX with a sufficient time resolution, oxidation and reduction reactions were induced with a nanosecond laser flash that synchronizes the entire ensemble of enzyme molecules (i.e., triggers simultaneous electron transfer by all molecules of the enzyme population). The first option (the flow-flash method) involves studying the kinetics of oxidation of the completely reduced enzyme (R state) by molecular oxygen in a single-turnover mode. To avoid the stage of mixing with oxygen becoming the limiting stage of the reaction, interaction with oxygen is triggered by photolysis of the preformed COX complex with the reduced BNC [69]. In the second case, electron is "injected" using photoactivated tris(bipyridine) ruthenium complex (Rubpy) into the enzyme that has previously been transferred to a state characterized by a particular extent of oxygen reduction in the BNC (O, P, or F) [70].

Although the second approach has been developed more recently than the flow-flash method, it was the first to be used in a combination with direct electrometry. It should be noted that electron injection into COX offers an important advantage, which is an ability to separate the sets of elementary stages of charge transfer associated with individual single-electron transitions in the catalytic cycle. In addition, COX oxidation by the oxygen molecule in the first approach occurs from the completely reduced state R (in which, in addition to BNC, the input redox centers are also in the reduced state), which is not observed under normal conditions. This review presents a detailed description of results obtained using electron injection by the photoactivated Rubpy complex (results

of the studies using the flow-flash method can be found in the brilliant reviews [71, 72]).

KINETICS OF MEMBRANE POTENTIAL GENERATION BY MITOCHONDRIAL COX

For the first time, the stages of charge translocation in the F → O transition of COX from bovine heart mitochondria were recorded by the joint efforts of the laboratories headed by A. D. Kaulen and A. A. Konstantinov [73, 74]. Electron transfer in the COX molecule was triggered by a single electron injection from the Rubpy complex induced with a laser flash. Later, the use of this technique has been extended to investigation of the COX molecules fixed in the P_M state (the third electron in the catalytic cycle; Fig. 2) and fully oxidized O state [63, 75, 76]. Several years after the time-resolved kinetics of the membrane potential generation by COX had been recorded at the Belozersky Institute of Physico-Chemical Biology, the Helsinki Bioenergetics Group developed an approach that used a combination of time-resolved electrometry and flow-flash method [77].

Electron injection into the F state (F → O_H transition) allowed to resolve three main components of the membrane potential generation by family A COXs [73, 74]. The "fast" microsecond phase (~40 μs) reflected electron transfer from Cu_A to heme *a*. The "medium" (~1 ms) and "slow" (~4 ms) components corresponded to the stages of vectorial proton transfer in the enzyme caused by the electron transfer from heme *a* to the BNC. Electron transfer between heme *a* and BNC normally occurs along the membrane, i.e., is non-electrogenic [22]. Electron injection from Rubpy into the P state of mitochondrial COX (P → F transition) was accompanied by a set of the $\Delta\Psi$ generation proton components that had a similar amplitude, but were somewhat faster [63], while photoreduction of oxidized COX (injection in the O state) was limited to the heme *a* reduction by Cu_A [63, 70, 76].

The total amplitudes of millisecond electrogenic components in the kinetics of potential generation for the P → F and F → O stages were similar (~80%), which led to the initial estimate of ~3 protons pumped through the membrane. Or ~1.5 pumped protons at each of the single-electron stages of the oxidative phase of the catalytic cycle [63, 73]. The amplitudes in the presteady-state measurements were estimated using the effect of membrane potential on the steady-state redox equilibrium between cytochrome *c* and heme *a* [78]. Based on this effect, the transfer of an electron from Cu_A to heme *a* (20% of photoelectric response; the "fast" component) is equivalent to the translocation of an elementary charge by ½ the value of the membrane dielectric barrier. Hence, the total amplitude of the millisecond proton phases (80%) is equivalent to the transmembrane translocation of two total charges, which would correspond to the transfer from the internal aqueous phase to the BNC of one proton by ½ of membrane thickness for protonation of the reduced oxygen atom ("substrate" proton) and coupled translocation of two "pumped" protons: one through the entire membrane and one more through ½ of its thickness [63, 73]. This assessment was consistent with the earlier conclusions obtained in the studies of the steady-state quasi-equilibrium reversal of the COX-catalyzed reaction in the coupled mitochondria. It was assumed that all four pumped protons can be transferred through the membrane during the catalytic cycle oxidative phase [79]. It was assumed that the reducing stage of the photocycle does not possess a sufficient supply of free energy and is not associated with the pumping of protons, which also followed from relatively low values of the BNC redox potentials under stationary conditions (in the O state) [80].

KINETICS OF MEMBRANE POTENTIAL GENERATION BY FAMILY A BACTERIAL COX ENZYMES

The use of direct electrometric method for studying the mechanism of COX activity has received further development due to site-directed mutagenesis of family A bacterial COXs, which are homologous to mitochondrial COXs. The most studied enzymes of this group are bacterial COXs of the aa_3 type from *R. sphaeroides* [15, 28, 30, 31, 45, 81, 82] and *P. denitrificans* [76, 83-86].

The studies of the F → O transition in the mutant aa_3-type COX from *R. sphaeroides* with the uncoupled phenotype (N139D substitution [30, 87, 88]) have resulted in the overestimation of the electrogenicity of the single-electron transitions in the oxidative phase of the COX catalytic cycle. The enzyme with the N139D mutation in the D channel fully retained its oxygen reductase activity in the steady-state measurements, but lost the ability to acidify the outer medium in the proteoliposome suspension (i.e., to pump protons across the membrane in the steady-state measurements). Generation of the membrane potential at the F → O stage in response to the electron injection in the mutant enzyme reflected translocation of one elementary charge through the membrane, namely, the transfer of an electron and a proton from the opposite sides of the membrane to the heme a_3 oxoferryl complex [30].

The ratio of the amplitudes of electrogenic components of the electron transfer from the outer side of the membrane [30, 31] and of the substrate proton transfer from the internal aqueous phase to the BNC in the N139D mutant allowed to estimate the electrogenic distance of heme *a* and BNC from the external aqueous phase (~0.4 of the membrane dielectric thickness), which was in good agreement with the structural data [32, 36].

Accordingly, the relative amplitude of the electrogenic phase, which reflects the transfer of the substrate proton in the N139D mutant from the internal aqueous phase to the BNC, was ~0.6 of the membrane dielectric thickness. The total amplitude of the "medium" and "slow" electrogenic phases in the P → F and F → O transitions in the wild-type COX and mitochondrial COX is ~4 times larger than the amplitude of the electrogenic phase of electron transfer from the outer side of the membrane to heme *a* [31, 63, 73], which is equivalent to the transfer of ~1.6 positive charge through the entire thickness of the membrane dielectric. That is, in addition to the transfer of one substrate proton from the internal aqueous phase to the BNC (~0.6 of the membrane dielectric thickness), additional electrogenic contribution to the single-electron transition in the wild-type COX, compared to the N139D mutant, corresponds to the transfer of approximately one proton through the membrane. In other words, both single-electron transitions in the oxidative phase of the COX catalytic cycle are associated with the transfer of one substrate proton to the BNC and pumping of no more than one proton through the membrane. Similar estimates were obtained for the P → F and F → O transitions in the reaction of fully reduced COX with oxygen using the electrometric method [89] and by measuring the protonation kinetics of a pH indicator [90].

Independently, Verkhovsky et al. [53] from the Helsinki Bioenergetics Group demonstrated that the total membrane potential generation in the reducing half-reaction of the COX catalytic cycle can involve not only the transfer of protons to the BNC, but also transmembrane pumping of protons. Later, the same group used a variant of the flow-flash method to oxidize fully reduced COX with an O_2 molecule in a single-turn mode followed by the electron injection from Rubpy. This approach allowed to study the kinetics of membrane potential generation associated with the single-electron reduction of the metastable oxidized state O_H of cytochrome oxidase. It was shown with time resolution [85, 86] that rapid oxidation of completely reduced COX was immediately followed by the short-lived oxidized state O_H characterized by a much more positive redox potential of BNC than the O state. In contrast to the O state, electron injection into COX in the O_H state was accompanied by rapid electron transfer to the BNC and associated stages of electrogenic proton translocation [65, 85, 86, 91, 92]. The characteristics of the electrogenic phases in the single-electron $O_H \rightarrow E_H$ transition [85, 86] generally resembled those for the transitions in the oxidative phase and are consistent with the transmembrane transfer of a single proton. Proton pumping during the $O_H \rightarrow E_H$ transition was also confirmed in the case of natural (and not artificial, like Rubpy) electron donor in the study of family A (subfamily A2) heme-copper oxidase *caa*$_3$ from *T. thermophilus*, which has an additional redox center (cytochrome *c*) and, accordingly, five electrons in a completely reduced state [11]. When the fully reduced *caa*$_3$ oxidase from *T. thermophilus* was oxidized by an oxygen molecule in the single-turnover mode, the final transition was the $O_H \rightarrow E_H$ transition [92]. The final electron acceptor in the $O_H \rightarrow E_H$ transition of this enzyme, as in the case of the artificial electron donor Rubpy, was Cu_B.

The $E_H \rightarrow R$ transition is presumably associated with the pumping of one proton. However, the stage of the second electron transfer in the COX catalytic cycle still remains the least studied process, since it was not possible to obtain a homogeneous population of enzyme molecules in the single-electron state (E_H). This is primarily due to the difficulty of fixing the enzyme in the E_H state and existence of multiple possible states of the single-electron (E and E_H) and oxidized (O and O_H) enzyme differing in their functional properties. Treating COX in the F state with carbon monoxide under steady-state conditions converted it to the E state, which has one electron equivalent more than the oxidized state O. Electron injection from Rubpy into this state led to a photoelectric response similar in its characteristics to the F → O transition [84]. However, electron distribution between the redox centers in the resulting E state differed significantly from the distribution observed for the E_H state formed by the electron injection from Rubpy into COX in the O_H state [65, 86, 92].

FUNCTIONAL ROLE OF PROTON-CONDUCTING PATHWAYS IN THE CATALYTIC CYCLE OF FAMILY A COX ENZYMES

The studies on the effect of mutations of proton-exchanging groups on the functional characteristics of the coupled proton transfer demonstrated that electrogenic translocation of protons by family A COX enzymes occurs through the proton-conducting structures ("channels" D and K) containing critical conserved proton-exchange residues [30, 31, 45, 81]. However, participation of these channels in the conduction of different protons at the individual stages of the catalytic cycle is organized in a non-trivial way. Based on the effect of mutations of particular amino acid residues [93, 94] and the three-dimensional structure of COX [32, 36], it was assumed that these two channels are specialized for conducting substrate protons (K channel) and protons pumped through the membrane (D channel).

If the D and K channels were responsible for the transfer of protons of different types, then mutations blocking their activity should have inhibited the F → O transition. However, while amino acid substitutions in the D channel suppressed the millisecond components of the potential generation and, therefore, electrogenic proton transfer at the F → O stage, the blockade of the K channel did not inhibit electrogenic proton transfer

at this stage [30, 31, 45, 81]. Moreover, in the presence of excess respiration substrates, i.e., when the influx of electrons was not the reaction rate-limiting stage, reduction of the BNC (O → R transition) in the K-channel mutants was hindered due to the blockade of proton capture from the matrix into the BNC during the reducing phase of the catalytic cycle. It was concluded that the D and K channels differ not in the nature of conducted protons (substrate or pumped), but in the type of the catalytic cycle half-reaction they serve [45, 81, 85].

Later experimental results indicated that the K channel does not appear to be involved in the transfer of pumped protons at all, while the D channel provides the transfer of substrate protons in the oxidative part of the cycle and all pumped protons in the catalytic cycle (as in oxidative phase and in the reducing phase). Indeed, if the transfer of pumped protons occurred through the K channel, then the N139D mutation in the D channel (which preserves the oxygen reductase function, but completely inhibits proton pumping through the membrane [30, 87]) should not affect the transfer of pumped protons in the reducing phase of the catalytic cycle. In accordance with this, no mutations in the K channel have been identified that specifically inhibited the pumping of protons across the membrane. It is currently accepted that the K channel transfers one or both substrate protons during the reducing part of the cycle (Fig. 2) [12, 85, 95]. It was found that the hydrogen bond between the hydroxyl group of the heme a_3 farnesyl substituent and redox-active tyrosine residue (Y288), which is present in the oxidized COX, was absent in the crystals of reduced COX form [40] and was replaced by water molecules (i.e., this bond can act as a "latch" in the upper part of the K channel).

The signal to turn off the K channel can be formation of the oxoferryl state of heme a_3 during generation of intermediate P in the A → P transition. The resulting oxene state of the oxygen atom (as a strong axial ligand of heme iron) can cause changes in the enzyme conformation, similar to the R → T transition in hemoglobin [45]. A slight shift of charges inside the K channel, which is closed in its upper part, can also occur during the oxidative half-reaction of the catalytic cycle [31, 82]. The role of such charge shift inside the channel is not clear; for example, it may lead to a decrease in the energy barrier for the electron transfer reactions inside the COX hydrophobic core.

Beside the D and K channels, mitochondrial COX might have the third proton pathway, the H channel, whose role in the conduction of protons remains a matter of debates [34, 96]. According to the authors of the study on the X-ray structural analysis of mammalian COXs [34, 35, 96], who identified this hypothetical proton pathway, the H channel conducts pumped protons into COX from the N side of the membrane through the vicinity of heme *a* to the D51 residue located near the P side of the membrane. The function of this channel and regulation of proton translocation through it, including physiological aspects of this regulation, have been poorly studied [14]. It was suggested that the H channel is involved in the conduction of pumped protons across the entire membrane [97]; according to other hypothesis, only the upper part of this pathway is used [98]. Finally, the third hypothesis states that the H channel is not involved in the proton pumping, but represents the so-called dielectric "well", whose role may be modulation of the redox potential of the nearby electron transfer, heme *a* [99, 100].

There are indications that mutations in the H channel inhibit proton translocation by the mitochondrial COX [34, 96]. However, targeted mutagenesis of enzymes from higher eukaryotes is technically difficult, which complicates interpretation of the obtained results [101]. At the same time, the exit portion of the proton H channel, whose conformational changes are the key element of the alternative hypothetical mechanism of proton pumping by the mitochondrial COX, is not conserved in homologous oxidases from bacteria [102, 103]. Moreover, mutations of homologous residues in the H channels of bacterial aa_3-type COXs do not inhibit these enzymes [103, 104]. The studies of COX proteins from lower eukaryotes (yeast) do not support involvement of the H channel in proton pumping [16].

MECHANISM OF MEMBRANE POTENTIAL GENERATION DURING THE SINGLE-ELECTRON TRANSITION F → O

Studying the effects of isotope substitution and zinc ions has been instrumental in the identification of electrogenic processes underlying the "medium" and "slow" phases of the membrane potential generation kinetics during the F → O transition. The effects of isotope substitution differ significantly between the electrogenic phases, which allowed to identify analogs of these phases in COX mutants and to correlate them with the transfer of different types of protons [30]. The "medium" phase was absent in the uncoupled mutant with the N139D substitution in the D channel, which retained the oxygen reductase activity but was unable to pump protons through the membrane. This suggests the association of the "medium" phase with the transfer of pumped proton, as well as that the pumped proton is translocated before the substrate one. Accordingly, the "slow" phase, which was retained in the mutant enzyme, is interpreted as the substrate proton transfer to the BNC.

In the presence of zinc ions (proton transport inhibitors) added externally to proteoliposomes with the mitochondrial COX or wild-type cytochrome aa_3 oxidase from *R. sphaeroides* [15, 105], the "slow" electrogenic phase decelerated. No such effect was observed

for the "medium" electrogenic phase. Zinc ions also had no impact on the protonic electrogenic phase in the uncoupled N139D mutant. Taken together, these data indicate that the "slow" electrogenic phase in the wild-type enzyme includes a stage of the pumped proton release to the membrane outer side and that this process is likely the rate-limiting reaction for the entire "slow" electrogenic phase [15]. In contrast to the proton entry pathways, the trajectory of proton exit to the outer membrane has been poorly studied. There are indications that the exit of water molecules is organized in a form of discrete trajectory through two channel-like structures that can also be involved in conducting the pumped proton to the outer side of the membrane [52, 106]. Studying the effects of different zinc concentrations on the kinetics of membrane potential generation in proteoliposomes with membrane-incorporated cytochrome aa_3 oxidase from *R. sphaeroides* indicated the presence of at least two separate effective binding sites for Zn^{2+} ions on the P side of the membrane. It was also shown that the release of the pumped proton from the proton loading site (PLS) of COX into the external aqueous phase can occur along several trajectories [15].

Analysis of the "medium" and "slow" phases using sequential reaction model revealed that the values of their relative amplitudes were close [107, 108]. Thus, the relative amplitudes of the "medium" and "slow" electrogenic protonic phases for the F → O transition in the mitochondrial enzyme were ~1.9-2.1 of the value for the "fast" electrogenic phase, i.e., which together corresponded to the transfer of two protons through most of the membrane dielectric [108]. As mentioned above, the D channel ensures the transfer of both pumped and substrate protons during transitions of the oxidative phase of the COX catalytic cycle [45, 81]. Therefore, the "medium" and "slow" electrogenic protonic phases can be interpreted as two sequential identical processes of reprotonation of some key residue located in the vicinity of the BNC in the D channel, with a minor contribution from other coupled charge transitions in the protein [107, 109, 110].

The conserved E286 residue located in the upper part of the D channel serves as an intermediate proton donor that ensures conduction of the pumped and substrate protons (Fig. 3). E286 is a bifurcation point in the translocation of protons through the D channel that can occur either along the substrate proton pathway to the heme a_3/Cu_B center or to the outer side of the membrane. Replacement of E286 with a non-protonatable analog (E286Q) inhibited the transfer of both pumped and substrate protons in the single-electron F → O transition [45, 81]. Experiments with the enzyme carrying the N139L mutation, which blocks the entrance to the D channel, allowed to identify the electrogenic stage of proton transfer from the putative primary proton donor (residue E286) to the BNC and to establish the electrogenic distance between them (~0.15 of thickness of the membrane dielectric) [31]. This is in good agreement with the structural data, according to which the distance from the internal aqueous phase to E286 is ~0.56 of the geometric thickness of the membrane [107]. In the case of proton deficiency in the D channel (deprotonated E286), the role of the proton donor for the BNC can be performed by the Y35 residue in the middle part of the channel [27].

Single-electron transition F → O in family A heme-copper oxidases upon electron injection from Rubpy begins with the reduction of Cu_A and electrogenic transfer of electron from Cu_A to heme *a* ("fast" component of the $\Delta\Psi$ generation kinetics) [17] (Fig. 3). A possible shift of the positive charge within the gated K channel in response to the heme *a* reduction may facilitate this process (step 2' in Fig. 3) [31]. Electron transfer from heme *a* to heme $a_3{}^{4+}{=}O^{2-}$ occurs along the membrane plane in almost electrically neutral manner. Proton translocation begins with the transfer of the pumped proton from E286 to the proton "trap" (PLS) located upstream of the BNC. In different family A heme-copper oxidases, heme a_3 propionate A and/or one of the histidine ligands of Cu_B can be considered as the PLS [111, 112]. There are indications that the role of PLS can belong to a cluster of proton-exchange groups, including propionates A and D of heme a_3 and nearby residues (D52 and K171 in mitochondrial COX) [113], or by the hydrophilic domain located above heme *a* [98].

In the F → O transition, the substrate proton is also transferred from E286 directly to the BNC, and E286 is reprotonated twice through the D channel during the entire transition. The "medium" electrogenic phase includes electrogenic proton transfer from E286 to the primary proton acceptor (PLS), as well as one of the successive electrogenic reprotonations of E286 from the internal aqueous N phase through the D channel (Fig. 3). The "slow" electrogenic phase involves the second reprotonation of E286 following the transfer from E286–COOH to the BNC of the proton involved in the oxygen chemical conversion.

There are indications that the proton transfer from E286 to the BNC (stage 5) is a part of the "slow" (in *R. sphaeroides* COX) or "medium" (in mitochondrial COX) electrogenic phases [28]. The transfer of the substrate proton to the BNC leads to the neutralization of transferred electron, the negative charge of which could stabilize the pumped proton located in the PLS. The transfer of a new proton deep into the membrane dielectric upon E286 reprotonation should lead to the electrostatic expulsion of the pumped proton from the PLS [112, 114, 115]. Accordingly, the "slow" electrogenic phase also involves proton release from the PLS to the outer side of the membrane, which can be slowed down by the addition of zinc ions from the P side of the membrane (Fig. 3).

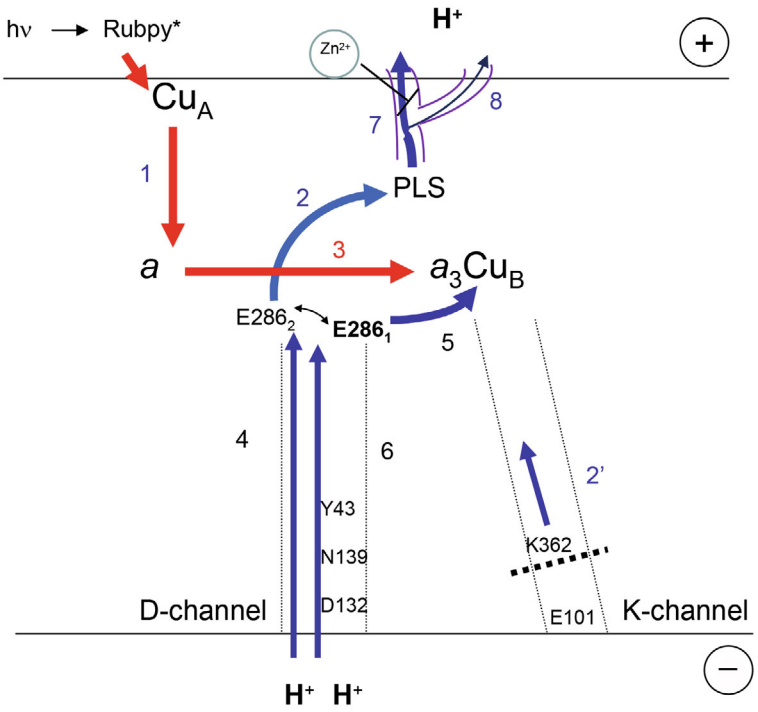

Fig. 3. The figure shows the electrogenic stages resolved by single-electron photoinjection using Rubpy in the F → O transition (transfer of the fourth electron in the COX catalytic cycle). Before the reaction begins, heme a_3 is in the oxoferryl state (not shown). Red arrows indicate directions of electron transfer; blue arrows indicate the stages of proton translocation. Two proton pathways (D and K channels) and their conserved amino acid residues are shown. Steps 1 and 3 reflect electron transfer from Cu_A to heme *a* and from heme *a* to the BNC, respectively. During the F → O transition, both protons (substrate and pumped) are transferred through the D channel. It is assumed that isomerization of E286 (transition between the $E286_1$ and $E286_2$ conformations) precedes proton transfer from E286 to the PLS. Individual stages of proton transfer are components of the "medium" (2 and 4) or the "slow" (6 and 7) electrogenic phases. An additional pathway for the pumped proton release from the PLS (step 8) was revealed in the presence of zinc ions [15]. Proton transfer from E286 to the BNC (step 5) is presumably a component of the "medium" (in mitochondrial COX) or "slow" (in *R. sphaeroides* COX) electrogenic phases. Stage 2' is a possible charge shift in the K channel in response to the heme *a* reduction [31].

THE USE OF DIRECT ELECTROMETRIC METHOD IN THE STUDIES OF FAMILY B HEME-COPPER OXIDASES

To understand the mechanism of coupled proton pumping by COX, it is important to study the diversity of heme-copper terminal oxidases [8], including enzymes of much less investigated and evolutionarily distant families B and C [19, 116, 117]. Although the studies of family B and C oxidases have started relatively recently, they have attracted a lot interest [29, 95, 118, 119]. To a great extent this is due to the common occurrence of these enzymes (along with copper-free *bd*-type oxidases) in pathogenic microorganisms and, therefore, their biomedical significance [120].

The use of direct electrometric method allowed to discover an interesting feature of the BNC from the ba_3-type COX from *T. thermophilus*, a typical representative of family B [121]. In the initial oxidized state, this enzyme does not react with exogenous ligands and, therefore, cannot be converted and stabilized in the P or F states by the treatment with hydrogen peroxide or carbon monoxide [121], as it was done for typical aa_3-type oxidases [63]. However, when an electron from Rubpy was injected into the fully oxidized (state O) COX ba_3 from *T. thermophilus* in the presence of hydrogen peroxide, an additional electrogenic reaction was observed, the rate of which was directly proportional to the concentration of the added peroxide. In other words, the BNC of this enzyme, which was inactive in the oxidized state toward external ligands, acquired the ability to bind ligands (and transit to the active/open state) in response to the single-electron injection and reduction of heme *b* [121].

An important aspect in the context of uniqueness and usefulness of direct electrometric method in the studies of the ba_3-type COX from *T. thermophilus* is that the average parameters of the catalytic cycle of this enzyme assessed by the degree of acidification of the outer compartment of proteoliposomes in the stationary oxygen reductase reaction, indicated the variability in the stoichiometry of proton pumping. Unlike family A oxidases, the stoichiometry of proton pumping by family B and C oxidases in the stationary measurements can vary within a significant range: from 0.5 to ~0.85 protons per electron (H^+/e^-) entering the BNC [66, 118, 121-124]. Application of direct electrometric method makes it possible to obtain and compare electrogenic parameters of individual single-electron transitions and to obtain

unique information about the features of the coupling mechanism.

In the ba_3-type COX from *T. thermophilus* (a typical representative of family B proteins), the stages of electrogenic proton transfer are resolved during the oxidative phase [122] and the first transition of the reducing phase of the catalytic cycle [66]. The stages during which electron transfer is not associated with the proton pumping across the membrane have been identified, which explained the decrease in the effective stoichiometry of proton pumping and its significant variability in family B oxidases [66, 122]. In particular, it was shown that in contrast to family A enzymes, one proton is pumped through the membrane instead of two in the oxidative phase of the catalytic cycle of ba_3-type COX from *T. thermophilus* [122]. At the same time, the transfer of the 1st electron in the reducing phase (transition $O_H \rightarrow E_H$) is also not associated with the proton pumping through the membrane, which can be caused by the membrane potential formation during the oxidative phase [66].

Apparently, family B enzymes have preserved only one functional proton entry channel, which is homologous to the K channel of family A oxidases [5, 29]. Using direct electrometric method, it was shown that in contrast to family A enzymes, family B oxidases use the K channel for the transfer of both substrate and pumped protons in the oxidative phase. The T315V mutation in the K-channel of ba_3-type COX from *T. thermophilus* causes a slowdown of the $F \rightarrow O_H$ transition due to the deceleration of the substrate proton transfer to the BNC, as well as uncoupling, i.e., complete absence of proton pumping in the oxidative phase of the catalytic cycle [29].

Funding. The study was supported by the Russian Science Foundation (project no. 23-24-00143).

Acknowledgments. The author would like to express his deepest gratitude to the untimely deceased A. A. Konstantinov, A. D. Kaulen, M. I. Verkhovsky, L. A. Drachev, and V. P. Skulachev. Collaboration with these outstanding scientists at different times has made an indelible impression on the author. The author is grateful to D. L. Zaslavsky, I. A. Smirnova, I. N. Belevich, Prof. M. Wikström and Prof. R. Gennis for collaboration in the studies of heme-copper oxidases by direct electrometric method.

Ethics declarations. The author declares no conflict of interest in financial or any other area. This article does not contain description of studies with human participants or animals performed by the author.

REFERENCES

1. Anraku, Y. (1988) Bacterial electron transport chains, *Ann. Rev. Biochem.*, **57**, 101-132, doi: 10.1146/annurev.bi.57.070188.000533.
2. Garcia-Horsman, J. A., Barquera, B., Rumbley, J., Ma, J., and Gennis, R. B. (1994) The superfamily of heme-copper respiratory oxidases, *J. Bacteriol.*, **176**, 5587-5600, doi: 10.1128/jb.176.18.5587-5600.1994.
3. Babcock, G. T., and Wikström, M. (1992) Oxygen Activation and the conservation of energy in cell respiration, *Nature*, **356**, 301-309, doi: 10.1038/356301a0.
4. Ferguson-Miller, S., and Babcock, G. T. (1996) Heme/copper terminal oxidases, *Chem. Rev.*, **7**, 2889-2907, doi: 10.1021/cr950051s.
5. Hemp, J., and Gennis, R. B. (2008) Diversity of the heme-copper superfamily in archaea: insights from genomics and structural modeling, *Results Probl. Cell Differ.*, **45**, 1-31, doi: 10.1007/400_2007_046.
6. Rich, P. R. (2017) Mitochondrial cytochrome *c* oxidase: catalysis, coupling and controversies, *Biochem. Soc. Trans.*, **45**, 813-829, doi: 10.1042/BST20160139.
7. Siletsky, S. A., and Borisov, V. B. (2021) Proton pumping and non-pumping terminal respiratory oxidases: active sites intermediates of these molecular machines and their derivatives, *Int. J. Mol. Sci.*, **22**, 10852, doi: 10.3390/ijms221910852.
8. Pereira, M. M., Santana, M., and Teixeira, M. (2001) A novel scenario for the evolution of haem-copper oxygen reductases, *Biochim. Biophys. Acta*, **1505**, 185-208, doi: 10.1016/S0005-2728(01)00169-4.
9. Yoshikawa, S., and Shimada, A. (2015) Reaction mechanism of cytochrome *c* oxidase, *Chem. Rev.*, **115**, 1936-1989, doi: 10.1021/cr500266a.
10. Fee, J. A., Yoshida, T., Surerus, K. K., and Mather, M. W. (1993) Cytochrome caa_3 from the thermophilic bacterium Thermus thermophilus: a member of the heme-copper oxidase superfamily, *J. Bioenerg. Biomembr.*, **25**, 103-114, doi: 10.1007/BF00762852.
11. Siletsky, S. A., Belevich, I., Soulimane, T., Verkhovsky, M. I., and Wikström, M. (2013) The fifth electron in the fully reduced caa_3 from *Thermus thermophilus* is competent in proton pumping, *Biochim. Biophys. Acta*, **1827**, 1-9, doi: 10.1016/j.bbabio.2012.09.013.
12. Wikström, M., Krab, K., and Sharma, V. (2018) Oxygen activation and energy conservation by cytochrome *c* oxidase, *Chem. Rev.*, **118**, 2469-2490, doi: 10.1021/acs.chemrev.7b00664.
13. Forte, E., Borisov, V. B., Siletsky, S. A., Petrosino, M., and Giuffre, A. (2019) In the respiratory chain of *Escherichia coli* cytochromes *bd*-I and *bd*-II are more sensitive to carbon monoxide inhibition than cytochrome bo_3, *Biochim. Biophys. Acta Bioenergetics*, **1860**, 148088, doi: 10.1016/j.bbabio.2019.148088.
14. Bjorck, M. L., Vilhjalmsdottir, J., Hartley, A. M., Meunier, B., Nasvik Ojemyr, L., Marechal, A., and Brzezinski, P. (2019) Proton-transfer pathways in the mitochondrial *S. cerevisiae* cytochrome *c* oxidase, *Sci. Rep.*, **9**, 20207, doi: 10.1038/s41598-019-56648-9.
15. Siletsky, S. A., and Gennis, R. B. (2021) Time-resolved electrometric study of the $F \rightarrow O$ transition in cytochrome *c*

oxidase. The effect of Zn^{2+} ions on the positive side of the membrane, *Biochemistry (Moscow)*, **86**, 105-122, doi: 10.1134/S0006297921010107.

16. Marechal, A., Xu, J. Y., Genko, N., Hartley, A. M., Haraux, F., Meunier, B., and Rich, P. R. (2020) A common coupling mechanism for A-type heme-copper oxidases from bacteria to mitochondria, *Proc. Natl. Acad. Sci. USA*, **117**, 9349-9355, doi: 10.1073/pnas.2001572117.
17. Siletsky, S. A. (2013) Steps of the coupled charge translocation in the catalytic cycle of cytochrome *c* oxidase, *Front. Biosci. (Landmark Ed)*, **18**, 36-57, doi: 10.2741/4086.
18. Fee, J. A., Sanders, D., Slutter, C. E., Doan, P. E., Aasa, R., Karpefors, M., and Vänngård, T. (1995) Multi-frequency epr evidence for a binuclear Cu_A center in cytochrome *c* oxidase: studies with a ^{63}Cu- and ^{65}Cu-enriched, soluble domain of the cytochrome ba_3, subunit II from *Thermus Thermophilus*, *Biochem. Biophys. Res. Commun.*, **212**, 77-83, doi: 10.1006/bbrc.1995.1938.
19. Soulimane, T., Buse, G., Bourenkov, G. B., Bartunik, H. D., Huber, R., and Than, M. E. (2000) Structure and mechanism of the aberrant ba_3-cytochrome *c* oxidase from *Thermus thermophilus*, *EMBO J.*, **19**, 1766-1776, doi: 10.1093/emboj/19.8.1766.
20. Pitcher, R. S., and Watmough, N. J. (2004) The bacterial cytochrome cbb_3 oxidases, *Biochim. Biophys. Acta*, **1655**, 388-399, doi: 10.1016/j.bbabio.2003.09.017.
21. Buschmann, S., Warkentin, E., Xie, H., Langer, J. D., Ermler, U., and Michel, H. (2010) The structure of cbb_3 cytochrome oxidase provides insights into proton pumping, *Science*, **329**, 327-330, doi: 10.1126/science.1187303.
22. Mitchell, P. (1968) *Chemiosmotic coupling and energy transduction*, Glynn Research Ltd., Bodmin.
23. Wikström, M. (1977) Proton pump coupled to cytochrome *c* oxidase in mitochondria, *Nature*, **266**, 271-273, doi: 10.1038/266271a0.
24. Wikström, M. (2004) Cytochrome c oxidase: 25 years of the elusive proton pump, *Biochim. Biophys. Acta*, **1655**, 241-247, doi: 10.1016/j.bbabio.2003.07.013.
25. Drachev, L. A., Jasaitis, A. A., Kaulen, A. D., Kondrashin, A. A., Liberman, E. A., Nemecek, I. B., Ostroumov, S. A., Semenov, A., and Skulachev, V. P. (1974) Direct measurement of electric current generation by cytochrome oxidase, H^+-ATPase and bacteriorhodopsin, *Nature*, **249**, 321-324, doi: 10.1038/249321a0.
26. Drachev, L. A., Kaulen, A. D., Khitrina, L. V., and Skulachev, V. P. (1981) Fast stages of photoelectric processes in biological membranes. I. Bacteriorhodopsin, *Eur. J. Biochem.*, **117**, 461-470, doi: 10.1111/j.1432-1033.1981.tb06361.x.
27. Belevich, I., Gorbikova, E., Belevich, N. P., Rauhamaki, V., Wikström, M., and Verkhovsky, M. I. (2010) Initiation of the proton pump of cytochrome *c* oxidase, *Proc. Natl. Acad. Sci. USA*, **107**, 18469-18474, doi: 10.1073/pnas.1010974107.
28. Siletsky, S. A., and Konstantinov, A. A. (2012) Cytochrome c oxidase: charge translocation coupled to single-electron partial steps of the catalytic cycle, *Biochim. Biophys. Acta*, **1817**, 476-488, doi: 10.1016/j.bbabio.2011.08.003.
29. Siletsky, S. A., Soulimane, T., Belevich, I., Gennis, R. B., and Wikström, M. (2021) Specific inhibition of proton pumping by the T315V mutation in the K channel of cytochrome ba_3 from *Thermus thermophilus*, *Biochim. Biophys. Acta Bioenergetics*, **1862**, 148450, doi: 10.1016/j.bbabio.2021.148450.
30. Siletsky, S. A., Pawate, A. S., Weiss, K., Gennis, R. B., and Konstantinov, A. A. (2004) Transmembrane charge separation during the ferryl-oxo → oxidized transition in a non-pumping mutant of cytochrome *c* oxidase, *J. Biol. Chem.*, **279**, 52558-52565, doi: 10.1074/jbc.M407549200.
31. Siletsky, S. A., Zhu, J., Gennis, R. B., and Konstantinov, A. A. (2010) Partial steps of charge translocation in the nonpumping N139L mutant of *Rhodobacter sphaeroides* cytochrome *c* oxidase with a blocked D-channel, *Biochemistry*, **49**, 3060-3073, doi: 10.1021/bi901719e.
32. Tsukihara, T., Aoyama, H., Yamashita, E., Takashi, T., Yamaguichi, H., Shinzawa-Itoh, K., Nakashima, R., Yaono, R., and Yoshikawa, S. (1996) The whole structure of the 13-subunit oxidized cytochrome *c* oxidase at 2.8 Å, *Science*, **272**, 1136-1144, doi: 10.1126/science.272.5265.1136.
33. Yoshikawa, S., Shinzawa-Itoh, K., Nakashima, R., Yaono, R., Inoue, N., Yao, M., Fei, M. J., Libeu, C. P., Mizushima, T., Yamaguchi, H., Tomizaki, T., and Tsukihara, T. (1998) Redox-coupled crystal structural changes in bovine heart cytochrome *c* oxidase, *Science*, **280**, 1723-1729, doi: 10.1126/science.280.5370.1723.
34. Tsukihara, T., Shimokata, K., Katayama, Y., Shimada, H., Muramoto, K., Aoyama, H., Mochizuki, M., Shinzawa-Itoh, K., Yamashita, E., Yao, M., Ishimura, Y., and Yoshikawa, S. (2003) The low-spin heme of cytochrome *c* oxidase as the driving element of the proton-pumping process, *Proc. Natl. Acad. Sci. USA*, **100**, 15304-15309, doi: 10.1073/pnas.2635097100.
35. Muramoto, K., Hirata, K., Shinzawa-Itoh, K., Yoko-o, S., Yamashita, E., Aoyama, H., Tsukihara, T., and Yoshikawa, S. (2007) A histidine residue acting as a controlling site for dioxygen reduction and proton pumping by cytochrome *c* oxidase, *Proc. Natl. Acad. Sci. USA*, **104**, 7881-7886, doi: 10.1073/pnas.0610031104.
36. Iwata, S., Ostermeier, C., Ludwig, B., and Michel, H. (1995) Structure at 2.8 Å resolution of cytochrome *c* oxidase from *Paracoccus denitrificans*, *Nature*, **376**, 660-669, doi: 10.1038/376660a0.
37. Ostermeier, C., Iwata, S., Ludwig, B., and Michel, H. (1995) F_V fragment-mediated crystallization of the membrane protein bacterial cytochrome *c* oxidase, *Nat. Struct. Biol.*, **2**, 842, doi: 10.1038/nsb1095-842.
38. Koepke, J., Olkhova, E., Angerer, H., Muller, H., Peng, G., and Michel, H. (2009) High resolution crystal structure of *Paracoccus denitrificans* cytochrome *c* oxidase: New insights into the active site and the proton

transfer pathways, *Biochim. Biophys. Acta*, **1787**, 635-645, doi: 10.1016/j.bbabio.2009.04.003.

39. Svensson-Ek, M., Abramson, J., Larsson, G., Tornroth, S., Brzezinski, P., and Iwata, S. (2002) The X-ray crystal structures of wild-type and EQ(I-286) mutant cytochrome *c* oxidases from *Rhodobacter sphaeroides*, *J. Mol. Biol.*, **321**, 329-339, doi: 10.1016/S0022-2836(02)00619-8.
40. Qin, L., Liu, J., Mills, D. A., Proshlyakov, D. A., Hiser, C., and Ferguson-Miller, S. (2009) Redox dependent conformational changes in cytochrome *c* oxidase suggest a gating mechanism for proton uptake, *Biochemistry*, **48**, 5121-5130, doi: 10.1021/bi9001387.
41. Abramson, J., Riistama, S., Larsson, G., Jasaitis, A., Svensson-Ek, M., Laakkonen, L., Puuustinen, A., Iwata, S., and Wikström, M. (2000) The structure of the ubiquinol oxidase from *Escherichia coli* and its ubiquinone binding site, *Nat. Struct. Biol.*, **7**, 910-917, doi: 10.1038/82824.
42. Noor, M. R., and Soulimane, T. (2013) Structure of $caa_{(3)}$ cytochrome *c* oxidase – a nature-made enzyme-substrate complex, *Biol. Chem.*, **394**, 579-591, doi: 10.1515/hsz-2012-0343.
43. Luna, V. M., Chen, Y., Fee, J. A., and Stout, C. D. (2008) Crystallographic studies of Xe and Kr binding within the large internal cavity of cytochrome ba_3 from *Thermus thermophilus*: structural analysis and role of oxygen transport channels in the heme-Cu oxidases, *Biochemistry*, **47**, 4657-4665, doi: 10.1021/bi800045y.
44. Fetter, J. R., Qian, J., Shapleigh, J., Thomas, J. W., Garcia-Horsman, A., Schmidt, E., Hosler, J., Babcock, G. T., Gennis, R. B., and Ferguson-Miller, S. (1995) Possible proton relay pathways in cytochrome *c* oxidase, *Proc. Natl. Acad. Sci. USA*, **92**, 1604-1608, doi: 10.1073/pnas.92.5.1604.
45. Konstantinov, A. A., Siletsky, S., Mitchell, D., Kaulen, A., and Gennis, R. B. (1997) The roles of the two proton input channels in cytochrome *c* oxidase from *Rhodobacter sphaeroides* probed by the effects of site-directed mutations on time resolved electrogenic intraprotein proton transfer, *Proc. Natl. Acad. Sci. USA*, **94**, 9085-9090, doi: 10.1073/pnas.94.17.9085.
46. Gennis, R. B. (1998) Multiple proton-conducting pathways in cytochrome oxidase and a proposed role for the active-site tyrosine, *Biochim. Biophys. Acta*, **1365**, 241-248, doi: 10.1016/S0005-2728(98)00075-9.
47. Branden, M., Tomson, F., Gennis, R. B., and Brzezinski, P. (2002) The entry point of the K-proton-transfer pathway in cytochrome *c* oxidase, *Biochemistry*, **41**, 10794-10798, doi: 10.1021/bi026093+.
48. Hofacker, I., and Schulten, K. (1998) Oxygen and proton pathways in cytochrome c oxidase, *Proteins: Struct. Funct.*, **30**, 100-107, doi: 10.1002/(SICI)1097-0134(199801)30:1<100::AID-PROT9>3.0.CO;2-S.
49. Popovic, D. M., and Stuchebrukhov, A. A. (2005) Proton exit channels in bovine cytochrome *c* oxidase, *J. Phys. Chem. B*, **109**, 1999-2006, doi: 10.1021/jp0464371.
50. Riistama, S., Puustinen, A., Verkhovsky, M. I., Morgan, J. E., and Wikström, M. (2000) Binding of O_2 and its reduction are both retarded by replacement of valine 279 by isoleucine in cytochrome *c* oxidase from *Paracoccus denitrificans*, *Biochemistry*, **39**, 6365-6372, doi: 10.1021/bi000123w.
51. Salomonsson, L., Lee, A., Gennis, R. B., and Brzezinski, P. (2004) A single-amino-acid lid renders a gas-tight compartment within a membrane-bound transporter, *Proc. Natl. Acad. Sci. USA*, **101**, 11617-11621, doi: 10.1073/pnas.0402242101.
52. Schmidt, B., McCracken, J., and Ferguson-Miller, S. (2003) A discrete water exit pathway in the membrane protein cytochrome *c* oxidase, *Proc. Natl. Acad. Sci. USA*, **100**, 15539-15542, doi: 10.1073/pnas.2633243100.
53. Verkhovsky, M. I., Jasaitis, A., Verkhovskaya, M. L., Morgan, L., and Wikström, M. (1999) Proton translocation by cytochrome *c* oxidase, *Nature*, **400**, 480-483, doi: 10.1038/22813.
54. Chance, B., Saronio, C., and Leigh, J. S., Jr. (1975) Functional intermediates in the reaction of membrane-bound cytochrome oxidase with oxygen, *J. Biol. Chem.*, **250**, 9226-9237, doi: 10.1016/S0021-9258(19)40634-0.
55. Hill, B. C., and Greenwood, C. (1983) Spectroscopic evidence for the participation of compound A ($Fe a_3^{2+}$-O_2) in the reaction of mixed-valence cytochrome *c* oxidase with oxygen at room temperature, *Biochem. J.*, **215**, 659-667, doi: 10.1042/bj2150659.
56. Muramoto, K., Ohta, K., Shinzawa-Itoh, K., Kanda, K., Taniguchi, M., Nabekura, H., Yamashita, E., Tsukihara, T., and Yoshikawa, S. (2010) Bovine cytochrome *c* oxidase structures enable O_2 reduction with minimization of reactive oxygens and provide a proton-pumping gate, *Proc. Natl. Acad. Sci. USA*, **107**, 7740-7745, doi: 10.1073/pnas.0910410107.
57. Kitagawa, T., and Ogura, T. (1997) Oxygen activation mechanism at the binuclear site of heme-copper oxidase superfamily as revealed by time-resolved resonance Raman spectroscopy, in *Progress in Inorganic Chemistry* (Karlin, K. D., ed) Wiley & Sons, pp. 431-479, doi: 10.1002/9780470166468.ch6.
58. Proshlyakov, D. A., Pressler, M. A., and Babcock, G. T. (1998) Dioxygen activation and bond cleavage by mixed-valence cytochrome *c* oxidase, *Proc. Natl. Acad.Sci. USA*, **95**, 8020-8025, doi: 10.1073/pnas.95.14.8020.
59. Proshlyakov, D. A., Pressler, M. A., DeMaso, C., Leykam, J. F., DeWitt, D. L., and Babcock, G. T. (2000) Oxygen activation and reduction in respiration: involvement of redox-active tyrosine 244, *Science*, **290**, 1588-1591, doi: 10.1126/science.290.5496.1588.
60. Buse, G., Soulimane, T., Dewor, M., Meyer, H. E., and Bloggel, M. (1999) Evidence for a copper coordinated histidine-tyrosine crosslink in the active site of cytochrome oxidase, *Protein Sci.*, **8**, 985-990, doi: 10.1110/ps.8.5.985.
61. Rauhamaki, V., Baumann, M., Soliymani, R., Puustinen, A., and Wikström, M. (2006) Identification

of histidin-tyrosin cross-link in the active site of the *cbb*$_3$-type cytochrome *c* oxidase from *Rhodobacter sphaeroides*, *Proc. Natl. Acad. Sci. USA*, **103**, 16135-16140, doi: 10.1073/pnas.0606254103.

62. Babcock, G. T. (1999) How oxygen is activated and reduced in respiration, *Proc. Natl. Acad. Sci. USA*, **96**, 12971-12973, doi: 10.1073/pnas.96.23.12971.
63. Siletsky, S., Kaulen, A. D., and Konstantinov, A. A. (1999) Resolution of electrogenic steps coupled to conversion of cytochrome *c* oxidase from the peroxy to the ferryl-oxo state, *Biochemistry*, **38**, 4853-4861, doi: 10.1021/bi982614a.
64. Sharma, V., Karlin, K. D., and Wikstrom, M. (2013) Computational study of the activated O_H state in the catalytic mechanism of cytochrome *c* oxidase, *Proc. Natl. Acad. Sci. USA*, **110**, 16844-16849, doi: 10.1073/pnas.1220379110.
65. Siletsky, S. A., Belevich, I., Wikström, M., Soulimane, T., and Verkhovsky, M. I. (2009) Time-resolved $O_H \rightarrow E_H$ transition of the aberrant *ba*$_3$ oxidase from *Thermus thermophilus*, *Biochim. Biophys. Acta*, **1787**, 201-205, doi: 10.1016/j.bbabio.2008.12.020.
66. Siletsky, S. A., Belevich, I., Belevich, N. P., Soulimane, T., and Wikström, M. (2017) Time-resolved generation of membrane potential by *ba*$_3$ cytochrome *c* oxidase from *Thermus thermophilus* coupled to single electron injection into the O and OH states, *Biochim. Biophys. Acta*, **1858**, 915-926, doi: 10.1016/j.bbabio.2017.08.007.
67. Siletsky, S. A., Mamedov, M. D., Lukashev, E. P., Balashov, S. P., Dolgikh, D. A., Rubin, A. B., Kirpichnikov, M. P., and Petrovskaya, L. E. (2016) Electrogenic steps of light-driven proton transport in ESR, a retinal protein from *Exiguobacterium sibiricum*, *Biochim. Biophys. Acta*, **1857**, 1741-1750, doi: 10.1016/j.bbabio.2016.08.004.
68. Kaulen, A. D. (2000) Electrogenic processes and protein conformational changes accompanying the bacteriorhodopsin photocycle, *Biochim. Biophys. Acta*, **1460**, 204-219, doi: 10.1016/S0005-2728(00)00140-7.
69. Gibson, Q. H., and Greenwood, C. (1963) Reactions of cytochrome oxidase with oxygen and carbon monoxide, *Biochem. J.*, **86**, 541-554, doi: 10.1042/bj0860541.
70. Nilsson, T. (1992) Photoinduced electron transfer from tris(2,2'-bipyridyl)ruthenium to cytochrome *c* oxidase, *Proc. Natl. Acad. Sci. USA*, **89**, 6497-6501, doi: 10.1073/pnas.89.14.6497.
71. Belevich, I., and Verkhovsky, M. I. (2008) Molecular mechanism of proton translocation by cytochrome *c* oxidase, *Antioxid. Redox Signal.*, **10**, 1-29, doi: 10.1089/ars.2007.1705.
72. Kaila, V. R., Verkhovsky, M. I., and Wikström, M. (2010) Proton-coupled electron transfer in cytochrome oxidase, *Chem. Rev.*, **110**, 7062-7081, doi: 10.1021/cr1002003.
73. Zaslavsky, D., Kaulen, A., Smirnova, I. A., Vygodina, T. V., and Konstantinov, A. A. (1993) Flash-induced membrane potential generation by cytochrome *c* oxidase, *FEBS Lett.*, **336**, 389-393, doi: 10.1016/0014-5793(93)80843-J.
74. Zaslavsky, D. L., Smirnova, I. A., Siletsky, S. A., Kaulen, A. D., Millett, F., and Konstantinov, A. A. (1995) Rapid kinetics of membrane potential generation by cytochrome *c* oxidase with the photoactive Ru(II)-tris-bipyridyl derivative of cytochrome *c* as electron donor, *FEBS Lett.*, **359**, 27-30, doi: 10.1016/0014-5793(94)01443-5.
75. Siletsky, S. A., Kaulen, A. D., and Konstantinov, A. A. (1997) Electrogenic events associated with peroxy- to ferryl-oxo state transition in cytochrome *c* oxidase, *Eur. J. Biophys.*, **26**, 98.
76. Verkhovsky, M. I., Tuukkanen, A., Backgren, C., Puustinen, A., and Wikström, M. (2001) Charge translocation coupled to electron injection into oxidized cytochrome *c* oxidase from *Paracoccus denitrificans*, *Biochemistry*, **40**, 7077-7083, doi: 10.1021/bi010030u.
77. Verkhovsky, M. I., Morgan, J. E., Verkhovskaya, M., and Wikström, M. (1997) Translocation of electrical charge during a single turnover of cytochrome *c* oxidase, *Biochim. Biophys. Acta*, **1318**, 6-10, doi: 10.1016/S0005-2728(96)00147-8.
78. Hinkle, P., and Mitchell, P. (1970) Effect of membrane potential on the redox poise between cytochrome *a* and cytochrome *c* in rat liver mitochondria, *J. Bioenerg.*, **1**, 45-60, doi: 10.1007/BF01516088.
79. Wikström, M. (1989) Identification of the electron transfers in cytochrome oxidase that are coupled to proton-pumping, *Nature*, **338**, 776-778, doi: 10.1038/338776a0.
80. Wikström, M., Krab, K., and Saraste, M. (1981) *Cytochrome Oxidase – A Synthesis*, Academic Press, New York.
81. Siletsky, S. A., Kaulen, A. D., Mitchell, D., Gennis, R. B., and Konstantinov, A. A. (1996) Resolution of two proton conduction pathways in cytochrome *c* oxidase, *EBEC Short Rep.*, **9**, 90.
82. Lepp, H., Svahn, E., Faxen, K., and Brzezinski, P. (2008) Charge transfer in the K proton pathway linked to electron transfer to the catalytic site in cytochrome *c* oxidase, *Biochemistry*, **47**, 4929-4935, doi: 10.1021/bi7024707.
83. Ruitenberg, M., Kannt, A., Bamberg, E., Ludwig, B., Michel, H., and Fendler, K. (2000) Single-electron reduction of the oxidized state is coupled to proton uptake via the K pathway in *Paracoccus denitrificans* cytochrome *c* oxidase, *Proc. Natl. Acad. Sci. USA*, **97**, 4632-4636, doi: 10.1073/pnas.080079097.
84. Ruitenberg, M., Kannt, A., Bamberg, E., Fendler, K., and Michel, H. (2002) Reduction of cytochrome *c* oxidase by a second electron leads to proton translocation, *Nature*, **417**, 99-102, doi: 10.1038/417099a.
85. Bloch, D., Belevich, I., Jasaitis, A., Ribacka, C., Puustinen, A., Verkhovsky, M. I., and Wikström, M. (2004) The catalytic cycle of cytochrome *c* oxidase is not the sum of its two halves, *Proc. Natl. Acad. Sci. USA*, **101**, 529-533, doi: 10.1073/pnas.0306036101.
86. Belevich, I., Bloch, D. A., Wikström, M., and Verkhovsky, M. I. (2007) Exploring the proton pump mechanism of cytochrome *c* oxidase in real time, *Proc. Natl. Acad. Sci. USA*, **104**, 2685-2690, doi: 10.1073/pnas.0608794104.

87. Pawate, A. S., Morgan, J., Namslauer, A., Mills, D., Brzezinski, P., Ferguson-Miller, S., and Gennis, R. B. (2002) A mutation in subunit I of cytochrome oxidase from *Rhodobacter sphaeroides* results in an increase in steady-state activity but completely eliminates proton pumping, *Biochemistry*, **41**, 13417-13423, doi: 10.1021/bi026582+.
88. Pfitzner, U., Hoffmeier, K., Harrenga, A., Kannt, A., Michel, H., Bamberg, E., Richter, O.-M. H., and Ludwig, B. (2000) Tracing the D-pathway in reconstituted site-directed mutants of cytochrome *c* oxidase from *Paracoccus denitrificans*, *Biochemistry*, **39**, 6756-6762, doi: 10.1021/bi992235x.
89. Ribacka, C., Verkhovsky, M. I., Belevich, I., Bloch, D. A., Puustinen, A., and Wikström, M. (2005) An elementary reaction step of the proton pump is revealed by mutation of tryptophan-164 to phenylalanine in cytochrome *c* oxidase from *Paracoccus denitrificans*, *Biochemistry*, **44**, 16502-16512, doi: 10.1021/bi0511336.
90. Faxen, K., Gilderson, G., Adelroth, P., and Brzezinski, P. (2005) A mechanistic principle for proton pumping by cytochrome *c* oxidase, *Nature*, **437**, 286-289, doi: 10.1038/nature03921.
91. Brand, S. E., Rajagukguk, S., Ganesan, K., Geren, L., Fabian, M., Han, D., Gennis, R. B., Durham, B., and Millett, F. (2007) A new ruthenium complex to study single-electron reduction of the pulsed O_H state of detergent-solubilized cytochrome oxidase, *Biochemistry*, **46**, 14610-14618, doi: 10.1021/bi701424d.
92. Siletsky, S. A., Belevich, I., Belevich, N. P., Soulimane, T., and Verkhovsky, M. I. (2011) Time-resolved single-turnover of caa_3 oxidase from *Thermus thermophilus*. Fifth electron of the fully reduced enzyme converts O_H into E_H state, *Biochim. Biophys. Acta*, **1807**, 1162-1169, doi: 10.1016/j.bbabio.2011.05.006.
93. Thomas, J. W., Puustinen, A., Alben, J. O., Gennis, R. B., and Wikström, M. (1993) Substitution of asparagine for aspartate-135 in subunit I of the cytochrome *bo* ubiquinol oxidase of *Escherichia coli* eliminates proton-pumping activity, *Biochemistry*, **32**, 10923-10928, doi: 10.1021/bi00091a048.
94. Garcia-Horsman, J. A., Puustinen, A., Gennis, R. B., and Wikström, M. (1995) Proton transfer in cytochrome bo_3 ubiquinol oxidase of *Escherichia coli*: second site mutations in subunit I that restore proton pumping in the decoupled mutant Asp135Asn, *Biochemistry*, **34**, 4428-4433, doi: 10.1021/bi00013a035.
95. Siletsky, S. A., Borisov, V. B., and Mamedov, M. D. (2017) Photosystem II and terminal respiratory oxidases: molecular machines operating in opposite directions, *Front. Biosci. (Landmark Ed)*, **22**, 1379-1426, doi: 10.2741/4550.
96. Shimokata, K., Katayama, Y., Murayama, H., Suematsu, M., Tsukihara, T., Muramoto, K., Aoyama, H., Yoshikawa, S., and Shimada, H. (2007) The proton pumping pathway of bovine heart cytochrome *c* oxidase, *Proc. Natl. Acad. Sci. USA*, **104**, 4200-4205, doi: 10.1073/pnas.0611627104.
97. Yoshikawa, S., Shimada, A., and Shinzawa-Itoh, K. (2015) Respiratory conservation of energy with dioxygen: cytochrome *c* oxidase, *Met. Ions Life Sci.*, **15**, 89-130, doi: 10.1007/978-3-319-12415-5_4.
98. Capitanio, N., Palese, L. L., Capitanio, G., Martino, P. L., Richter, O. M., Ludwig, B., and Papa, S. (2012) Allosteric interactions and proton conducting pathways in proton pumping $aa_{(3)}$ oxidases: heme a as a key coupling element, *Biochim. Biophys. Acta*, **1817**, 558-566, doi: 10.1016/j.bbabio.2011.11.003.
99. Rich, P. R., and Marechal, A. (2013) Functions of the hydrophilic channels in protonmotive cytochrome *c* oxidase, *J. R. Soc. Interface*, **10**, 20130183, doi: 10.1098/rsif.2013.0183.
100. Sharma, V., Jambrina, P. G., Kaukonen, M., Rosta, E., and Rich, P. R. (2017) Insights into functions of the H channel of cytochrome *c* oxidase from atomistic molecular dynamics simulations, *Proc. Natl. Acad. Sci. USA*, **114**, E10339-E10348, doi: 10.1073/pnas.1708628114.
101. Wikström, M., and Verkhovsky, M. I. (2007) Mechanism and energetics of proton translocation by the respiratory heme-copper oxidases, *Biochim. Biophys. Acta*, **1767**, 1200-1214, doi: 10.1016/j.bbabio.2007.06.008.
102. Salje, J., Ludwig, B., and Richter, O.-M. H. (2005) Is a third proton-conducting pathway operative in bacterial cytochrome *c* oxidase? *Biochem. Soc. Trans.*, **33**, 829-831, doi: 10.1042/BST0330829.
103. Lee, H.-m., Das, T. K., Rousseau, D. L., Mills, D., Fergusson-Miller, S., and Gennis, R. (2000) Mutations in the putative H-channel in the cytochrome *c* oxidase from *Rhodobacter sphaeroides* show that this channel is not important for proton conduction but reveals modulation of the properties of heme *a*, *Biochemistry*, **39**, 2989-2996, doi: 10.1021/bi9924821.
104. Pfitzner, U., Odenwald, A., Ostermann, T., Weingard, L., Ludwig, B., and Richter, O. M. H. (1998) Cytochrome *c* oxidase (heme aa_3) from *Paracoccus denitrificans*: analysis of mutations in putative proton channels of subunit I, *J. Bioenerg. Biomembr.*, **30**, 89-97, doi: 10.1023/A:1020515713103.
105. Kuznetsova, S. S., Azarkina, N. V., Vygodina, T. V., Siletsky, S. A., and Konstantinov, A. A. (2005) Zink ions as cytochrome *c* oxidase inhibitors: two sites of action, *Biochemistry (Moscow)*, **70**, 128-136, doi: 10.1007/s10541-005-0091-6.
106. Sugitani, R., and Stuchebrukhov, A. A. (2009) Molecular dynamics simulation of water in cytochrome c oxidase reveals two water exit pathways and the mechanism of transport, *Biochim. Biophys. Acta*, **1787**, 1140-1150, doi: 10.1016/j.bbabio.2009.04.004.
107. Medvedev, D. M., Medvedev, E. S., Kotelnikov, A. I., and Stuchebrukhov, A. A. (2005) Analysis of the kinetics of the membrane potential generated by cytochrome *c* oxidase upon single electron injection, *Biochim. Biophys. Acta*, **1710**, 47-56, doi: 10.1016/j.bbabio.2005.08.008.
108. Siletsky, S., and Konstantinov, A. A. (2006) Electrogenic mechanism of cytochrome *c* oxidase, *The 8th European Biological Chemistry Conference*, p. 80.

109. Siletsky, S. A., Han, D., Brand, S., Morgan, J. E., Fabian, M., Geren, L., Millett, F., Durham, B., Konstantinov, A. A., and Gennis, R. B. (2006) Single-electron photoreduction of the P_M intermediate of cytochrome *c* oxidase, *Biochim. Biophys. Acta*, **1757**, 1122-1132, doi: 10.1016/j.bbabio.2006.07.003.
110. Sugitani, R., Medvedev, E. S., and Stuchebrukhov, A. A. (2008) Theoretical and computational analysis of the membrane potential generated by cytochrome *c* oxidase upon single electron injection into the enzyme, *Biochim. Biophys. Acta*, **1777**, 1129-1139, doi: 10.1016/j.bbabio.2008.05.006.
111. Kaila, V. R., Sharma, V., and Wikström, M. (2011) The identity of the transient proton loading site of the proton-pumping mechanism of cytochrome *c* oxidase, *Biochim. Biophys. Acta*, **1807**, 80-84, doi: 10.1016/j.bbabio.2010.08.014.
112. Popovic, D. M., and Stuchebryukhov, A. A. (2004) Proton pumping mechanism and catalytic cycle of cytochrome *c* oxidase: Coulomb pump model with kinetic gating, *FEBS Lett.*, **566**, 126-130, doi: 10.1016/j.febslet.2004.04.016.
113. Lu, J., and Gunner, M. R. (2014) Characterizing the proton loading site in cytochrome *c* oxidase, *Proc. Natl. Acad. Sci. USA*, **111**, 12414-12419, doi: 10.1073/pnas.1407187111.
114. Rich, P. R. (1995) Towards an understanding of the chemistry of oxygen reduction and proton translocation in the iron-copper respiratory oxidases, *Aust. J. Plant Physiol.*, **22**, 479-486, doi: 10.1071/PP9950479.
115. Wikström, M., and Sharma, V. (2018) Proton pumping by cytochrome *c* oxidase – a 40 year anniversary, *Biochim. Biophys. Acta Bioenergetics*, **1859**, 692-698, doi: 10.1016/j.bbabio.2018.03.009.
116. Zimmermann, B. H., Nitsche, C. I., Fee, J. A., Rusnak, F., and Munck, E. (1988) Properties of a copper-containing cytochrome ba_3: a second terminal oxidase from the extreme thermophile *Thermus Thermophilus*, *Proc. Natl. Acad. Sci. USA*, **85**, 5779-5783, doi: 10.1073/pnas.85.16.5779.
117. Rauhamaki, V., Bloch, D. A., Verkhovsky, M. I., and Wikström, M. (2009) Active site of cytochrome cbb_3, *J. Biol. Chem.*, **284**, 11301-11308, doi: 10.1074/jbc.M808839200.
118. Rauhamaki, V., Bloch, D. A., and Wikström, M. (2012) Mechanistic stoichiometry of proton translocation by cytochrome cbb_3, *Proc. Natl. Acad. Sci. USA*, **109**, 7286-7291, doi: 10.1073/pnas.1202151109.
119. Steimle, S., van Eeuwen, T., Ozturk, Y., Kim, H. J., Braitbard, M., Selamoglu, N., Garcia, B. A., Schneidman-Duhovny, D., Murakami, K., and Daldal, F. (2021) Cryo-EM structures of engineered active bc_1-cbb_3 type $CIII_2CIV$ super-complexes and electronic communication between the complexes, *Nat. Commun.*, **12**, 929, doi: 10.1038/s41467-021-21051-4.
120. Borisov, V. B., Siletsky, S. A., Nastasi, M. R., and Forte, E. (2021) ROS defense systems and terminal oxidases in bacteria, *Antioxidants (Basel)*, **10**, 839, doi: 10.3390/antiox10060839.
121. Siletskiy, S., Soulimane, T., Azarkina, N., Vygodina, T. V., Buse, G., Kaulen, A., and Konstantinov, A. (1999) Time-resolved generation of membrane potential by ba_3 cytochrome *c* oxidase from *Thermus thermophilus*. Evidence for reduction-induced opening of the binuclear centre, *FEBS Lett.*, **457**, 98-102, doi: 10.1016/S0014-5793(99)01019-4.
122. Siletsky, S. A., Belevich, I., Jasaitis, A., Konstantinov, A. A., Wikström, M., Soulimane, T., and Verkhovsky, M. I. (2007) Time-resolved single-turnover of ba_3 oxidase from *Thermus thermophilus*, *Biochim. Biophys. Acta*, **1767**, 1383-1392, doi: 10.1016/j.bbabio.2007.09.010.
123. Kannt, A., Lancaster, C. R., and Michel, H. (1998) The coupling of electron transfer and proton translocation: electrostatic calculations on *Paracocus denitrificans* cytochrome *c* oxidase, *Biophys. J.*, **74**, 708-721, doi: 10.1016/S0006-3495(98)73996-7.
124. Rauhamaki, V., and Wikström, M. (2014) The causes of reduced proton-pumping efficiency in type B and C respiratory heme-copper oxidases, and in some mutated variants of type A, *Biochim. Biophys. Acta*, **1837**, 999-1003, doi: 10.1016/j.bbabio.2014.02.020.